Nuclear Physics **A505** (1989) 448–470
North-Holland, Amsterdam

COULOMB EXCITATION IN INTERMEDIATE-ENERGY COLLISIONS

A.N.F. ALEIXO and C.A. BERTULANI

Instituto de Física, Universidade Federal do Rio de Janeiro, 21945 Rio de Janeiro, RJ, Brazil

Received 24 May 1989
(Revised 21 July 1989)

Abstract: We study the interplay between retardation and Coulomb recoil in the theory of Coulomb excitation of heavy ions at bombarding energies around 100 MeV/nucleon. A semiclassical calculation with relativistically corrected trajectories and a full expansion of the electromagnetic propagator is performed. At these energies Coulomb excitation of giant resonances become dominant and the cross sections for it are very large, especially at grazing collisions. A comparison with the non-relativistic and with the relativistic calculations is made, showing that in intermediate-energy collisions neither of those reproduce the correct values of the cross sections.

1. Introduction

The excitation of a nucleus by means of the electromagnetic interaction with another nucleus is known as Coulomb excitation. Since the interaction strength is proportional to the charge Z of the projectile nucleus, Coulomb excitation is especially useful in the collision of heavy ions, with cross sections proportional to Z^2. One can make sure that one has pure Coulomb excitation by keeping the bombarding energy below the Coulomb barrier. Indeed, this has been used for many years for the study of electromagnetic properties of low-lying nuclear states [1]).

The probability for Coulomb exciting a nuclear state $|f\rangle$ from an initial state $|i\rangle$ becomes larger the longer the transition time $t_{fi} = \hbar/(E_f - E_i) = 1/\omega_{fi}$ is comparable with the interaction time $t_{coll} = a/v$, in a heavy-ion collision with half-distance of closest approach a and projectile velocity v. Otherwise, the nucleus responds adiabatically to the interaction. That is, the cross section for Coulomb excitation is large if the *adiabaticity parameter* satisfies the condition

$$\zeta = \frac{t_{coll}}{t_{fi}} = \omega_{fi}\frac{a}{v} < 1 . \tag{1.1}$$

This *adiabatic condition* limits the possible excitation energies to be below 1–2 MeV in sub-barrier collisions.

A possible way to overcome this limitation, and to excite higher-lying states, is to increase the projectile energy. In this case, the shortest distance at which the nuclei still interact only electromagnetically is of the order of the sum of the nuclear

radii, $R = R_P + R_T$. At very high energies one has also to take into account the relativistic contraction by means of the Lorentz factor

$$\gamma = (1 - v^2/c^2)^{-1/2}, \tag{1.2}$$

with c being the velocity of light. That is, in a collision with impact parameter R, the interaction time is of the order of $R/\gamma v$. For such a collision the adiabaticity condition (1.1) becomes

$$\xi(R) = \frac{\omega_{fi} R}{\gamma v} < 1 . \tag{1.3}$$

From this relation one obtains that, for heavy-ion collisions at bombarding energies above 100 MeV/nucleon, states with energy up to 10–20 MeV can be readily excited.

The theory of low-energy Coulomb excitation is very well settled [1]) and has been used for several decades to infer many properties of nuclear structure. The standard semiclassical theory of Coulomb excitation at low energies [1]) assumes that the relative motion takes place on a classical Rutherford trajectory, and the cross section for exciting a definite state $|f\rangle$ from the state $|i\rangle$ is then given by

$$\left(\frac{d\sigma}{d\Omega}\right)_{i\to f} = \left(\frac{d\sigma}{d\Omega}\right)_{Ruth} P_{i\to f} \tag{1.4}$$

where $P_{i\to f}$ is the probability of exciting the target by means of the time-dependent electromagnetic field of the projectile.

In the case of relativistic heavy-ion collisions pure Coulomb excitation may be distinguished from other processes, by demanding extreme forward scattering and avoiding collisions in which violent reactions take place [2]). The Coulomb excitation of relativistic heavy ions is thus characterized by straight-line trajectories with impact parameter b larger than the sum of the radii of the two colliding ions. A detailed calculation of relativistic electromagnetic excitation along this basis was performed by Winther and Alder [3]). As in the non-relativistic case, they showed how one can separate the contributions of the several electric ($E\lambda$) and magnetic ($M\lambda$) multipolarities to the excitation.

Recently, a new interest both in the experiment and in the theory of relativistic Coulomb excitation appeared [see ref. [4]) and references therein]. Experimentally, with the high-energy machines operating in CERN and in Brookhaven, one studies several processes in which Coulomb excitation plays a much more important role than the contribution from strong interactions. These processes are mainly the excitation of giant resonances in the colliding nuclei, which normally leads to fission, or to particle emission.

In the intermediate-energy regime, around 100 MeV per nucleon, Coulomb excitation of giant resonances is also a subject of increasing interest. Bertrand and collaborators [5]) have measured the inelastic scattering of ^{17}O on ^{208}Pb at a bombarding energy of 84 MeV/nucleon with the GANIL Accelerator. They found that the

cross sections for the excitation of giant resonant structures are very large (2 b/sr), and that the spectra are dominated by Coulomb excitation of the isovector giant dipole resonance (IVGDR) and the isoscalar giant quadrupole resonance (ISGQR). Their results demonstrate that inelastic scattering at medium energies (~100 MeV/nucleon) can be an important tool in the study of both isovector and isoscalar giant resonances.

The semiclassical theory of Coulomb excitation in low-energy collisions accounts for the Rutherford bending of the trajectory, but relativistic retardation effects are neglected [1]). On the other hand, in the theory of relativistic Coulomb excitation recoil effects on the trajectory are neglected (one assumes straight-line motion) but retardation is handled correctly. In fact, the onset of retardation brings new important effects, such as the steady increase of the excitation cross sections with bombarding energy. In a heavy-ion collision around 100 MeV/nucleon the Lorentz factor γ is about 1.1. Since this factor enters the excitation cross sections in many ways, like in the adiabaticity parameter (1.3), one expects that some sizeable modifications in the theory of relativistic Coulomb excitation should occur. Recoil corrections are not negligible either, and the relativistic calculations based on the straight-line parametrization should not be completely appropriate to describe the excitation probabilities and cross sections. The Coulomb recoil in a single collision is of the order of

$$a_0 = \frac{Z_P Z_T e^2}{m_0 v^2}, \tag{1.5}$$

which is the well-known *half-distance of closest approach* in a head-on collision, with m_0 equal to the reduced mass of the colliding nuclei. Although this recoil is small for intermediate-energy collisions, the excitation probabilities are quite sensitive to it. This is important for example in the excitation of giant resonances, because the adiabaticity parameter is of the order of one (see eq. 1.3). When $\xi(b) \ll 1$, the excitation probabilities depends on b approximately like $1/b^2$, while when $\xi(b)$ becomes greater than one it has a $e^{-2\pi\xi(b)}/b^2$ behaviour. Therefore, when $\xi \approx 1$ a slight change of b may vary the excitation probabilities appreciably.

It was suggested in ref. [6]) that an interpolation between the non-relativistic and the relativistic Coulomb excitation theory would be reasonable to describe Coulomb excitation in intermediate-energy collisions, where both recoil and retardation effects are present. Nonetheless, the actual calculation leading to such interpolated values was not performed. A salient feature of their results is that if one uses the relativistic Coulomb excitation theory for all bombarding energies, the calculated excitation cross sections are much larger than the expected correct values for projectile energies below ~200 MeV/nucleon. This can be readily understood, since the relativistic calculation neglects recoil and, their extrapolation to low-energy collisions, considers that the ions stay close much longer than they actually do. As a consequence, this increases the excitation probability. On the other hand, if one uses the low-energy

Coulomb excitation theory for all bombarding energies one finds that the excitation cross sections are much smaller than what they should be for energies greater than ~50 MeV/nucleon [ref. [6])]. This arises because retardation, which is not included in the non-relativistic calculations, increases the strength of the Coulomb interaction and consequently the excitation probabilities.

In fact, as we shall show in the next sections, in the bombarding energy range 50–200 MeV one must include both retardation and recoil effects. This can be accomplished in a straightforward way in the semiclassical approach with a simplified relativistic trajectory, appropriate for heavy-ion collisions, and the full expansion of the electromagnetic propagator.

This paper is organized as follows. In sect. 2 we describe the classical trajectory appropriate for intermediate-energy heavy-ion collisions, to be used in the calculation of the excitation amplitudes. Sect. 3 deals with the multipole expansion of the excitation amplitudes accounting for retardation effects. The calculation follows the same approach as the one followed in the non-relativistic case. Inclusion of retardation leads to the appearance of extra terms and functions in the orbital integrals. In sect. 4 the cross sections are calculated and written as a product of a kinematical factor (the equivalent photon numbers) and a dynamical one, involving the matrix elements for electromagnetic transition in a nucleus. A comparison among the low- and the high-energy limits of the calculation is done in sect. 5, together with applications to some reactions. Our conclusions and summary are presented in sect. 6.

2. The classical trajectory

In the semiclassical theory of Coulomb excitation the nuclei are assumed to follow classical trajectories and the excitation probabilities are calculated in time-dependent perturbation theory. At low energies one assumes Rutherford trajectories for the relative motion, while at relativistic energies one assumes straight-line motion. In intermediate-energy collisions, where one wants to account for recoil and retardation simultaneously, one should solve the general classical problem of the motion of two relativistic charged particles. But, even if radiation is neglected, this problem can only be solved if one particle has infinite mass [7]). This approximation should be sufficient if we take, e.g. the collision $^{16}O+^{208}Pb$ as our system. An improved solution may be obtained by use of the reduced mass, as we indicate below.

In the classical one-body problem, one starts with the relativistic lagrangian

$$\mathscr{L} = -m_0 c^2 \left\{ 1 - \frac{1}{c^2}(\dot{r}^2 + r^2\dot{\phi}^2) \right\}^{1/2} - \frac{Z_P Z_T e^2}{r}, \tag{2.1}$$

where $\dot{r}$ and $\dot{\phi}$ are the radial and the angular velocity of the particle, respectively (see fig. 1). Using the Euler–Lagrange equations one finds three kinds of solutions, depending on the sign of the charges and the angular momentum in the collision.

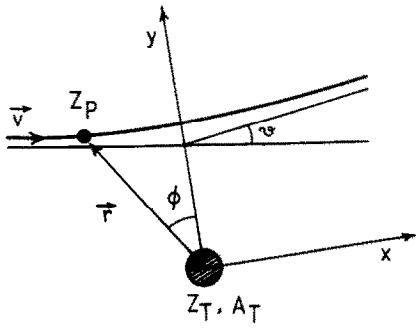

Fig. 1. Classical Coulomb scattering of a charged particle by another, infinitely-heavy one. The system of axes used in text is shown. The deflection angle is denoted by ϑ.

In the case of our interest, the appropriate solution relating the collisional angle ϕ and the distance r between the nuclei is [7])

$$\frac{1}{r} = A[\epsilon \cos W\phi - 1], \tag{2.2}$$

where

$$W = \left[1 - \left(\frac{Z_P Z_T e^2}{cL_0}\right)^2\right]^{1/2}, \tag{2.3a}$$

$$A = \frac{Z_P Z_T e^2 E}{c^2 L_0^2 W^2}, \tag{2.3b}$$

$$\epsilon = \frac{cL_0}{Z_P Z_T e^2 E}\left[E^2 - m_0^2 c^4 + \left(\frac{m_0 c Z_P Z_T e^2}{L_0}\right)^2\right]^{1/2}. \tag{2.3c}$$

E is the total bombarding energy in MeV, m_0 is the mass of the particle and L_0 its angular momentum. In terms of the Lorentz factor γ and of the impact parameter b, $E = \gamma m_0 c^2$ and $L_0 = \gamma m_0 v b$. The above solution is valid if $L_0 > Z_P Z_T e^2/c$. In heavy-ion collisions at intermediate energies one has $L_0 \gg Z_P Z_T e^2/c$ for impact parameters that do not lead to strong interactions. It is also easy to show that, from the magnitudes of the parameters involved in heavy-ion collisions at intermediate energies, the trajectory (2.2) can be very well described by approximating

$$W = 1, \quad A = \frac{a_0}{\gamma b^2}, \qquad \epsilon = \sqrt{\frac{b^2\gamma^2}{a_0^2} + 1}, \tag{2.4}$$

where a_0 is half the distance of closest approach in a head-on collision (if the nuclei were pointlike and if non-relativistic kinematics were used), and ϵ is the excentricity parameter. In the approximation (2.4) b is related to the deflection angle ϑ by $b = (a_0/\gamma)\cot\frac{1}{2}\vartheta$. In the case of heavy-ion collisions at intermediate energies, the error in the deflection angle that one finds by using these approximations is less than 0.1%.

The time dependence for a particle moving along the trajectory (2.2) may be directly obtained by solving the equation of angular momentum conservation. Introducing the parametrization

$$r(\chi) = \frac{a_0}{\gamma}[\epsilon \cosh \chi + 1] \tag{2.5}$$

we find

$$t = \frac{a_0}{\gamma v}[\chi + \epsilon \sinh \chi]\,. \tag{2.6}$$

Using the scattering plane perpendicular to the z-axis, one finds that the corresponding components of $\boldsymbol{r}$ may be written as

$$x = a[\cosh \chi + \epsilon]\,, \tag{2.7a}$$

$$y = a\sqrt{\epsilon^2 - 1}\,\sinh \chi\,, \tag{2.7b}$$

$$z = 0\,, \tag{2.7c}$$

where $a = a_0/\gamma$. This parametrization is of the same form as commonly used in the non-relativistic case [1]), except that a_0 is substituted by $a_0/\gamma \equiv a$. Since in general $a \ll b$, one might assume that a good approximation to describe Coulomb excitation at intermediate energies would be a rescaling of the impact parameter b which appears in the analytical expressions of the theory of relativistic Coulomb excitation. The reason is that the excitation occurs most probably when the nuclei are closer along the trajectory. But then they are displaced by an extra distance of order of a_0/γ due to Coulomb repulsion. Nonetheless, this recoil correction enters the orbital integrals for Coulomb excitation in a delicate way. Winther and Alder [3]) have shown, by means of an analysis of the orbital integrals in the non-relativistic case for large angular momenta (large impact parameter), that a reasonable approximation is a rescaling the form

$$b \to b + \frac{\pi a_0}{2\gamma} \tag{2.8}$$

in the analytical expressions for relativistic Coulomb excitation. This rescaling averages the contributions of all impact parameters around the straight-line value b. In section 5 we shall make a comparison of the relativistic expressions, improved by this correction, with the semiclassical calculation based on the trajectories parametrized by eq. (2.7).

As we quoted before, the classical solution for the relative motion of two relativistic charges interacting electromagnetically can only be solved analytically if radiation is neglected, and if one of the particles has infinite mass. Non-relativistically this problem is solvable by the introduction of centre-of-mass and relative-motion coordinates. Then, the result is equivalent to that of a particle with reduced mass

$m_0 = m_P m_T/(m_P + m_T)$ under the action of the same potential. The particle with reduced mass m_0 is lighter than those with mass m_P and m_T, and this accounts for the simultaneous recoil of them. An exact relativistic solution should reproduce this behaviour as the relative-motion energy is lowered. We shall use the reduced mass definition of m_0 as usual in the parametrization of the classical trajectory of Coulomb excitation in intermediate-energy collisions, as outlined above. In a $^{16}O + ^{208}Pb$ collision this is not a too serious approximation. For heavier systems like U + U it would be the simplest way to overcome this difficulty. But, as energy increases, this approximation is again unimportant since the trajectories will be straight lines, parametrized by an impact parameter b. Therefore, the parametrization of the classical trajectory as given by eq. (2.7) with a reduced-mass particle, besides reproducing both the non-relativistic and the relativistic energies, must give a resonable solution to the kind of collisions we want to study.

In the next section we shall formulate the theory of Coulomb excitation for intermediate-energy collisions, where such questions are relevant, using the parametrization of the trajectory as given by eq. (2.7). Then, we make a comparison with what one expects from the non-relativistic and relativistic Coulomb excitation formulas [1,3,4]).

3. Excitation amplitudes

The amplitude for Coulomb excitation of a target from the initial state $|i\rangle$ to the final state $|f\rangle$ is given in first-order time-dependent perturbation theory by

$$a_{fi} = \frac{1}{i\hbar} \int \left\{ \rho_{fi}(\boldsymbol{r}) \phi(\omega, \boldsymbol{r}) + \frac{1}{c} \boldsymbol{j}_{fi}(\boldsymbol{r}) \cdot \boldsymbol{A}(\omega, \boldsymbol{r}) \right\} d^3 r \tag{3.1}$$

where $\rho_{fi}(\boldsymbol{j}_{fi})$ is the nuclear transition density (current) and

$$\phi(\omega, \boldsymbol{r}) = Z_P e \int_{-\infty}^{\infty} e^{i\omega t} \frac{e^{i\kappa|\boldsymbol{r} - \boldsymbol{r}'(t)|}}{|\boldsymbol{r} - \boldsymbol{r}'(t)|} dt, \tag{3.2a}$$

$$\boldsymbol{A}(\omega, \boldsymbol{r}) = \frac{Z_P e}{c} \int_{-\infty}^{\infty} \boldsymbol{v}'(t) e^{i\omega t} \frac{e^{i\kappa|\boldsymbol{r} - \boldsymbol{r}'(t)|}}{|\boldsymbol{r} - \boldsymbol{r}'(t)|} dt, \tag{3.2b}$$

are the retarded potentials generated by a projectile with charge Z_P following a Coulomb trajectory. The frequency ω is given in terms of the initial, E_i, and final, E_f, energies of the excited nucleus as

$$\hbar\omega = E_f - E_i \tag{3.3}$$

and $\kappa = \omega/c$. The magnitude of the amplitudes (3.1) will be small compared to unity for the situations we shall study. Therefore, use of first-order perturbation theory is justified.

Using the continuity equation for the nuclear transition current, expanding $\phi(\omega, \boldsymbol{r})$ and $\boldsymbol{A}(\omega, \boldsymbol{r})$ into multipoles and assuming that the nuclei do not interpenetrate, one obtains

$$a_{\mathrm{fi}} = \frac{Z_{\mathrm{P}} e}{i\hbar} \sum_{\lambda\mu} \frac{4\pi}{2\lambda+1} (-1)^{\mu} \{S(\mathrm{E}\lambda, \mu)\mathcal{M}(\mathrm{E}\lambda, -\mu) + S(\mathrm{M}\lambda, \mu)\mathcal{M}(\mathrm{M}\lambda, -\mu)\} \tag{3.4}$$

where $\mathcal{M}(\pi\lambda, \mu)$ are the matrix elements for electromagnetic transitions, defined as

$$\mathcal{M}(\mathrm{E}\lambda, \mu) = \frac{(2\lambda+1)!!}{\kappa^{\lambda+1} c(\lambda+1)} \int \boldsymbol{j}_{\mathrm{fi}}(\boldsymbol{r}) \cdot \boldsymbol{\nabla} \times \boldsymbol{L}\{j_{\lambda}(\kappa r) Y_{\lambda\mu}(\theta, \phi)\} \, \mathrm{d}^3 r, \tag{3.5a}$$

$$\mathcal{M}(\mathrm{M}\lambda, \mu) = -\frac{i(2\lambda+1)!!}{\kappa^{\lambda} c(\lambda+1)} \int \boldsymbol{j}_{\mathrm{fi}}(\boldsymbol{r}) \cdot \boldsymbol{L}\{j_{\lambda}(\kappa r) Y_{\lambda\mu}(\theta, \phi)\} \, \mathrm{d}^3 r \tag{3.5b}$$

with $\boldsymbol{L} = -i\boldsymbol{r} \times \boldsymbol{\nabla}$.

The orbital integrals $S(\pi\lambda, \mu)$ are given by

$$S(\mathrm{E}\lambda, \mu) = -\frac{i\kappa^{\lambda+1}}{\lambda(2\lambda-1)!!} \int_{-\infty}^{\infty} \frac{\partial}{\partial r'} \{r'(t) h_{\lambda}^{(1)}[\kappa r'(t)]\} Y_{\lambda\mu}[\theta'(t), \phi'(t)] \, \mathrm{e}^{i\omega t} \, \mathrm{d}t$$
$$- \frac{\kappa^{\lambda+2}}{c\lambda(2\lambda-1)!!} \int_{-\infty}^{\infty} \boldsymbol{v}'(t) \cdot \boldsymbol{r}'(t) h_{\lambda}^{(1)}[\kappa r'(t)] Y_{\lambda\mu}[\theta'(t), \phi'(t)] \, \mathrm{e}^{i\omega t} \, \mathrm{d}t, \tag{3.6a}$$

$$S(\mathrm{M}\lambda, \mu) = -\frac{i}{\gamma m_0 c} \frac{\kappa^{\lambda+1}}{\lambda(2\lambda-1)!!}$$
$$\times \boldsymbol{L}_0 \cdot \int_{-\infty}^{\infty} \boldsymbol{\nabla}'\{h_{\lambda}^{(1)}[\kappa r'(t)] Y_{\lambda\mu}[\theta'(t), \phi'(t)]\} \, \mathrm{e}^{i\omega t} \, \mathrm{d}t \tag{3.6b}$$

where $\boldsymbol{L}_0$ is the angular momentum of relative motion, which is constant:

$$L_0 = \gamma a m_0 v \cot\tfrac{1}{2}\vartheta, \tag{3.7}$$

with ϑ equal to the (centre-of-mass) scattering angle. The $h_{\lambda}^{(1)}(x)$ are first-order spherical Hankel functions [8]). In non-relativistic collisions

$$\kappa r' = \frac{\omega r'}{c} = \frac{v}{c} \frac{\omega r'}{v} < \frac{v}{c} \ll 1 \tag{3.8}$$

because when the relative distance r' obeys the relations $\omega r'/v \geq 1$ the interaction becomes adiabatic. Then one uses the limiting form of $h_{\lambda}^{(1)}$ for small values of its argument [8]) to show that

$$S^{\mathrm{NR}}(\mathrm{E}\lambda, \mu) \approx \int_{-\infty}^{\infty} r'^{-\lambda-1}(t) Y_{\lambda\mu}\{\theta'(t), \phi'(t)\} \, \mathrm{e}^{i\omega t} \, \mathrm{d}t, \tag{3.9a}$$

$$S^{\mathrm{NR}}(\mathrm{M}\lambda, \mu) \approx -\frac{1}{\lambda m_0 c} \boldsymbol{L}_0 \cdot \int_{-\infty}^{\infty} \boldsymbol{\nabla}'\{r'^{-\lambda-1}(t) Y_{\lambda\mu}[\theta'(t), \phi'(t)]\} \, \mathrm{e}^{i\omega t} \, \mathrm{d}t, \tag{3.9b}$$

which are the usual orbital integrals in the non-relativistic Coulomb excitation theory with hyperbolic trajectories (see eqs. II.A.43 of ref. [1])).

In the intermediate-energy case the relation (3.8) is partially relaxed (of course, for relativistic energies, $v \sim c$, it is not valid) and one has to keep the more complex form (3.6) for the orbital integrals.

Using the z-axis perpendicular to the trajectory plane, the recursion relations for the spherical Hankel functions*, and the identity

$$\boldsymbol{v}\cdot\boldsymbol{r}=\frac{\mathrm{d}\chi}{\mathrm{d}t}\otimes\frac{\mathrm{d}\boldsymbol{r}}{\mathrm{d}\chi}\cdot\boldsymbol{r}=a\epsilon v\sinh\chi, \tag{3.10}$$

we can rewrite the orbital integrals, in terms of the parametrization (2.6) and (2.7), as

$$\begin{aligned}S(\mathrm{E}\lambda,\mu)=&-\frac{i\kappa^{\lambda}\eta}{c\lambda(2\lambda-1)!!}\mathscr{C}_{\lambda\mu}\int_{-\infty}^{\infty}\mathrm{d}\chi\,\mathrm{e}^{i\eta(\epsilon\sinh\chi+\chi)}\\&\times\frac{(\epsilon+\cosh\chi+i\sqrt{\epsilon^2-1}\sinh\chi)^{\mu}}{(\epsilon\cosh\chi+1)^{\mu-1}}\\&\times\left[(\lambda+1)h_{\lambda}-\frac{v\eta}{c}(\epsilon\cosh\chi+1)h_{\lambda+1}+i\left(\frac{v}{c}\right)^{2}\eta\epsilon h_{\lambda}\sinh\chi\right]\end{aligned} \tag{3.11}$$

where

$$\mathscr{C}_{\lambda\mu}=\begin{cases}\sqrt{\dfrac{2\lambda+1}{4\pi}}\dfrac{\sqrt{(\lambda-\mu)!(\lambda+\mu)!}}{(\lambda-\mu)!!(\lambda+\mu)!!}(-1)^{(\lambda+\mu)/2}, & \text{for } \lambda+\mu=\text{even}\\ 0, & \text{for } \lambda+\mu=\text{odd},\end{cases} \tag{3.12}$$

$$\eta=\frac{\omega a}{v}=\frac{\omega a_0}{\gamma v}, \tag{3.13}$$

and with all h_{λ}'s as functions of $(v/c)\eta\ (\epsilon\cosh\chi+1)$.

For convenience, we define

$$I(\mathrm{E}\lambda,\mu)=\frac{va^{\lambda}}{\mathscr{C}_{\lambda\mu}}S(\mathrm{E}\lambda,\mu) \tag{3.14}$$

and we translate the path of integration by an amount $\frac{1}{2}i\pi$ to avoid strong oscillations of the integrand. We find,

$$\begin{aligned}I(\mathrm{E}\lambda,\mu)=&-i\left(\frac{v\eta}{c}\right)^{\lambda+1}\frac{1}{\lambda(2\lambda-1)!!}\mathrm{e}^{-\pi\eta/2}\int_{-\infty}^{\infty}\mathrm{d}\chi\,\mathrm{e}^{-\eta\epsilon\cosh\chi}\,\mathrm{e}^{i\eta\chi}\\&\times\frac{(\epsilon+i\sinh\chi-\sqrt{\epsilon^2-1}\cosh\chi)^{\mu}}{(i\epsilon\sinh\chi+1)^{\mu-1}}\\&\times\left[(\lambda+1)h_{\lambda}-zh_{\lambda+1}-\left(\frac{v}{c}\right)^{2}\epsilon\eta h_{\lambda}\cosh\chi\right]\end{aligned} \tag{3.15}$$

* From now on we shall drop the index 1 of the Hankel functions, being clear that they are the first-order ones.

where all h_λ's are now functions of

$$z = \frac{v}{c}\eta(i\epsilon \sinh\chi + 1). \tag{3.16}$$

In the case of magnetic excitations, one may explore the fact that $\boldsymbol{L}_0$ is perpendicular to the scattering plane to show that

$$\frac{1}{m_0}\boldsymbol{L}_0\cdot\boldsymbol{\nabla}\{h_\lambda(\kappa r)\,Y_{\lambda\mu}(\tfrac{1}{2}\pi,\phi)\} = \gamma\frac{av}{r}\cot\tfrac{1}{2}\vartheta\sqrt{\frac{2\lambda+1}{2\lambda+3}}\sqrt{(\lambda+1)^2-\mu^2}$$
$$\times\mathscr{C}_{\lambda+1,\mu}\,e^{i\mu\phi}\,h_\lambda(\kappa r).$$

The magnetic orbital integrals become

$$S(M\lambda,\mu) = -ia\frac{v}{c}\frac{\kappa^{\lambda+1}}{\lambda(2\lambda-1)!!}\sqrt{\frac{2\lambda+1}{2\lambda+3}}\sqrt{(\lambda+1)^2-\mu^2}$$
$$\times\mathscr{C}_{\lambda+1,\mu}\cot\tfrac{1}{2}\vartheta\int_{-\infty}^{\infty}h_\lambda[\kappa r'(t)]\frac{1}{r'(t)}e^{i\mu\phi'(t)}e^{i\omega t}\,dt. \tag{3.17}$$

Defining,

$$I(M\lambda,\mu) = -\frac{\lambda c a^\lambda S(M\lambda,\mu)}{\mathscr{C}_{\lambda+1,\mu}\cot\tfrac{1}{2}\vartheta}\{[(2\lambda+1)/(2\lambda+3)][(\lambda+1)^2-\mu^2]\}^{-1/2} \tag{3.18}$$

we obtain, using the parametrization (2.6) and (2.7), and translating the integral path by $\frac{1}{2}i\pi$,

$$I(M\lambda,\mu) = \frac{i(v\eta/c)^{\lambda+1}}{(2\lambda-1)!!}e^{-\pi\eta/2}\int_{-\infty}^{\infty}d\chi\,h_\lambda(z)\,e^{-\eta\epsilon\cosh\chi}$$
$$\times e^{i\eta\chi}\frac{(\epsilon+i\sinh\chi-\sqrt{\epsilon^2-1}\cosh\chi)^\mu}{(i\epsilon\sinh\chi+1)^\mu}. \tag{3.19}$$

Generally, the most important magnetic excitation has M1 multipolarity.

4. Cross sections and equivalent photon numbers

The square modulus of eq. (3.4) gives the probability of exciting the target nucleus from the initial state $|I_iM_i\rangle$ to the final state $|I_fM_f\rangle$ in a collision with c.m. scattering angle ϑ. If the orientation of the initial state is not specified, the cross section for exciting the nuclear state of spin I_f is

$$d\sigma_{i\to f} = \frac{a^2\epsilon^4}{4}\frac{1}{2I_i+1}\sum_{M_i,M_f}|a_{fi}|^2\,d\Omega, \tag{4.1}$$

where $\frac{1}{4}a^2\epsilon^4 \mathrm{d}\Omega$ is the elastic (Rutherford) cross section. Using the Wigner-Eckart theorem and the orthogonality properties of the Clebsch-Gordan coefficients, one can show that

$$\frac{\mathrm{d}\sigma_{\mathrm{i}\to\mathrm{f}}}{\mathrm{d}\Omega} = \frac{4\pi^2 Z_{\mathrm{P}}^2 e^2}{\hbar^2} a^2\epsilon^4 \sum_{\lambda\mu} \frac{B(\pi\lambda, I_{\mathrm{i}}\to I_{\mathrm{f}})}{(2\lambda+1)^3} |S(\pi\lambda, \mu)|^2 \tag{4.2}$$

where $\pi = \mathrm{E}$ or M stands for the electric or magnetic multipolarity, and

$$B(\pi\lambda, I_{\mathrm{i}}\to I_{\mathrm{f}}) = \frac{1}{2I_{\mathrm{i}}+1} \sum_{M_{\mathrm{i}}, M_{\mathrm{f}}} |\mathcal{M}(\pi\lambda, \mu)|^2 \tag{4.3}$$

is the reduced transition probability.

Integration of (4.2) over all energy transfers $\varepsilon = \hbar\omega$, and summation over all possible final states of the projectile nucleus leads to

$$\frac{\mathrm{d}\sigma_{\mathrm{C}}}{\mathrm{d}\Omega} = \sum_{\mathrm{f}} \int \frac{\mathrm{d}\sigma_{\mathrm{i}\to\mathrm{f}}}{\mathrm{d}\Omega} \rho_{\mathrm{f}}(\varepsilon)\, \mathrm{d}\varepsilon \tag{4.4}$$

where $\rho_{\mathrm{f}}(\varepsilon)$ is the density of final states of the target with energy $E_{\mathrm{f}} = E_{\mathrm{i}} + \varepsilon$. Inserting (4.2) into (4.4) one finds

$$\frac{\mathrm{d}\sigma_{\mathrm{C}}}{\mathrm{d}\Omega} = \sum_{\pi\lambda} \frac{\mathrm{d}\sigma_{\pi\lambda}}{\mathrm{d}\Omega} = \sum_{\pi\lambda} \int \frac{\mathrm{d}\varepsilon}{\varepsilon} \frac{\mathrm{d}n_{\pi\lambda}}{\mathrm{d}\Omega}(\varepsilon)\sigma_\gamma^{\pi\lambda}(\varepsilon)\,, \tag{4.5a}$$

where

$$\sigma_\gamma^{\pi\lambda}(\varepsilon) = \frac{(2\pi)^3(\lambda+1)}{\lambda[(2\lambda+1)!!]^2} \sum_{\mathrm{f}} \rho_{\mathrm{f}}(\varepsilon)\kappa^{2\lambda-1} B(\pi\lambda, I_{\mathrm{i}}\to I_{\mathrm{f}}) \tag{4.5b}$$

are the photonuclear absorption cross sections for a given multipolarity $\pi\lambda$. The total photonuclear cross section is a sum of all these multipolarities,

$$\sigma_\gamma = \sum_{\pi\lambda} \sigma_\gamma^{\pi\lambda}(\varepsilon)\,. \tag{4.5c}$$

The functions $n_{\pi\lambda}(\varepsilon)$ are called the *equivalent photon numbers* [4]), and are given by

$$\frac{\mathrm{d}n_{\pi\lambda}}{\mathrm{d}\Omega} = \frac{Z_{\mathrm{P}}^2\alpha}{2\pi} \frac{\lambda[(2\lambda+1)!!]^2}{(\lambda+1)(2\lambda+1)^3} \frac{c^2a^2\epsilon^4}{\kappa^{2(\lambda-1)}} \sum_{\mu} |S(\pi\lambda, \mu)|^2\,, \tag{4.6}$$

where α is the fine-structure constant. Since all nuclear excitation dynamics is contained in the photoabsorption cross section, the equivalent photon numbers (4.6) do not depend on the nuclear structure. They are kinematical factors, depending on the orbital motion. They may be interpreted as the number of equivalent (virtual) photons that hit the target per unit (solid) scattering angle. The usefulness of Coulomb excitation, even in first-order processes, is displayed in eq. (4.5a). The field of a real photon contains all multipolarities with the same weight and the photonuclear cross section (4.5c) is a mixture of the contributions from all multipolarities, although only a few contribute in most processes. In the case of Coulomb

excitation the total cross section is weighted by kinematical factors which are different for each projectile or bombarding energy. This allows one to disentangle the multipolarities when several ones are involved in the excitation process.

In terms of the orbital integrals $I(\mathrm{E}\lambda, \mu)$, given by (3.15), and using the eqs. (3.14) and (3.11), we find for the electric multipolarities

$$\frac{\mathrm{d}n_{\mathrm{E}\lambda}}{\mathrm{d}\Omega} = \frac{Z_{\mathrm{P}}^2\alpha}{8\pi^2}\left(\frac{c}{v}\right)^{2\lambda} \frac{\lambda[(2\lambda+1)!!]^2}{(\lambda+1)(2\lambda+1)^2}\,\epsilon^4\eta^{-2\lambda+2}$$

$$\times \sum_{\substack{\mu \\ \lambda+\mu=\text{even}}} \frac{(\lambda-\mu)!(\lambda+\mu)!}{[(\lambda-\mu)!!(\lambda+\mu)!!]^2}\,|I(\mathrm{E}\lambda, \mu)|^2 . \tag{4.7}$$

In the case of magnetic excitations we find

$$\frac{\mathrm{d}n_{\mathrm{M}\lambda}}{\mathrm{d}\Omega} = \frac{Z_{\mathrm{P}}^2\alpha}{8\pi^2}\left(\frac{c}{v}\right)^{2(\lambda-1)} \frac{[(2\lambda+1)!!]^2}{\lambda(\lambda+1)(2\lambda+1)^2}\,\eta^{-2\lambda+2}\epsilon^4(\epsilon^2-1)$$

$$\times \sum_{\substack{\mu \\ \lambda+\mu=\text{odd}}} \frac{[(\lambda+1)^2-\mu^2](\lambda+1-\mu)!(\lambda+1+\mu)!}{[(\lambda+1-\mu)!!(\lambda+1+\mu)!!]^2}\,|I(\mathrm{M}\lambda, \mu)|^2 . \tag{4.8}$$

Since the impact parameter is related to the scattering angle by $b = a\cot\frac{1}{2}\vartheta$, we can also write

$$\frac{\mathrm{d}n_{\pi\lambda}}{2\pi b\,\mathrm{d}b} = \frac{4}{a^2\epsilon^4}\,\frac{\mathrm{d}n_{\pi\lambda}}{\mathrm{d}\Omega}, \tag{4.9}$$

which are interpreted as the number of equivalent photons of frequency ω, incident on the target per unit area, in a collision with impact parameter b.

The concept of the equivalent photon numbers is very useful, especially in relativistic collisions. In these collisions the momentum and the energy transfer due to the Coulomb interaction are related by $\Delta p = \Delta E/v \approx \Delta E/c$. This means that the virtual photons are almost real. One usually explores this fact to extract information about real photon processes from the reactions induced by relativistic charges, and vice versa. This is the basis of the Weizsäcker-Williams method, commonly used to calculate cross sections for Coulomb excitation, particle production, bremsstrahlung, etc. (see e.g. ref. [4])). In the case of Coulomb excitation, even at low energies, although the equivalent photon numbers should not be interpreted as (almost) real ones, the cross sections can still be written as a product of them and the cross sections induced by real photons. This happens because the excitation occurs in a divergence-free field (in contrast to electron scattering), since it is assumed from the beginning that the nuclei do not interpenetrate. Then the matrix elements for the excitation contain only the transverse components of the electromagnetic field, and turn out to be the same as those appearing in photoexcitation of the nuclei.

This allows one to extract information about photonuclear processes by means of measurements on Coulomb excitation, even at low- and intermediate-energy collisions, with the advantage that one has access to processes which could hardly be performed by using real photons like, e.g. multiple excitation. Recently [6]), it has been proposed the study of radiative capture cross sections of interest in astrophysics by means of an unfolding of the Coulomb breakup of light nuclei incident on a target with large Z. As seen from the projectile, the target provides a large amount of equivalent photons which lead to its disruption. In principle such experiments are easier to perform than the radiative-capture cross-section measurements at the extremely low relative energies required for astrophysical studies [6]).

5. Results and comparisons

Using the eqs. (4.7) and (4.8), we make an analysis of Coulomb excitation extending from low- to high-energy collisions. As an example, we study the excitations induced by ^{16}O in $^{16}O+^{208}Pb$ collisions. Since the expression (4.6) is quite general, valid for all energies, under the assumption that the nuclei do not overlap, the equivalent photon numbers contain all information about the differences among the low and the high-energy scattering.

In figs. 2, 3 and 4 we show $dn_{\pi\lambda}/2\pi b\, db$, for the E1 (fig. 2), E2 (fig. 3), and M1 (fig. 4) multipolarities, and for the collision $^{16}O+^{208}$ Pb with an impact parameter $b = 15$ fm. They are the equivalent photon numbers with frequency $\omega = 10$ MeV/$\hbar$ incident on ^{208}Pb. The dotted lines are obtained by using the non-relativistic eq. (A.1) of the appendix, while the dashed lines correspond to the relativistic expressions (A.3a–c) of the appendix. One observes that the relativistic expressions overestimate the equivalent photon numbers at low energies, while the non-relativistic expressions underestimate them at high energies. The most correct values are given by the solid lines, calculated according to eqs. (4.7) and (4.8). They reproduce the low- and the high-energy limits, giving an improved interpolation between these limits at intermediate energies. These discrepancies are more apparent for the E1 and the E2 multipolarities. In the energy interval around 100 MeV/nucleon neither the low-energy theory nor the high-energy one can reproduce well the correct values. This energy interval is indeed very sensitive to the effects of retardation and of Coulomb recoil.

In order to illustrate more clearly the errors one obtains by the use of the low and the high energy theories, extended to the intermediate energy, we plot in fig. 5 the relative difference

$$\Delta_{\pi\lambda} = \left| 1 - \frac{dn_{\pi\lambda}^{\mathrm{RorNR}}}{dn_{\pi\lambda}} \right| \tag{5.1}$$

for the E1 (fig. 5a) and the E2 (fig. 5b) multipolarity, as a function of the excitation energy, and at 100 MeV/nucleon. By $n_{\pi\lambda}^{\mathrm{NR}}$ ($n_{\pi\lambda}^{\mathrm{R}}$) we mean the equivalent photon

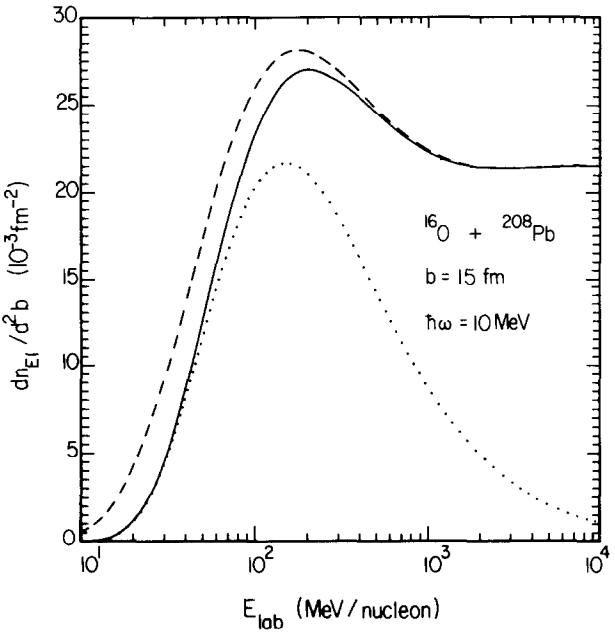

Fig. 2. Electric dipole number of equivalent photons per unit area $d^2b \equiv 2\pi b\, db$, with energy of 10 MeV, incident on ^{208}Pb in a collision with ^{16}O at impact parameter $b = 15$ fm, and as a function of the bombarding energy in MeV per nucleon. The dotted line and the dashed line correspond to calculations performed with the non-relativistic and with the relativistic approaches, respectively. The solid line represents a more correct calculation, as described in the text.

numbers calculated within the non-relativistic (relativistic) formalism. We observe that the relative error is approximately constant for $\hbar\omega < 10$ MeV, being larger (around 15%) when one uses the non-relativistic than when one uses the relativistic theory. These discrepancies increase sharply when one reaches the excitation energy of $\hbar\omega > 10$ MeV. The reason is that, for such excitation energies, the adiabaticity factor of eq. (1.3) becomes greater than unity ($\xi > 1$). This means that excitation energies of order of 10 MeV (like in the case of giant resonance excitation) are in the transition region from a constant behaviour of the equivalent photon numbers to that of an exponential ($\sim e^{-\pi\xi}$) decay. This is more transparent in fig. 6 where we plot the equivalent photon numbers for $E_{lab} = 100$ MeV/nucleon, $b = 15$ fm, and as a function of $\hbar\omega$. One also observes from this figure that the E2 multipolarity component of the electromagnetic field dominates at low frequencies. Nonetheless, over the range of $\hbar\omega$ up to some tens of MeV, the E2 matrix elements of excitation are much smaller than the E1 elements for most nuclei, and the E2 effects become unimportant. However, such effects are relevant for the excitation of the isoscalar E2 giant resonance (ISGQR) which have large matrix elements.

Winther and Alder indicated a simple way to account for recoil corrections in the theory of relativistic Coulomb excitation. This was done by a comparison among

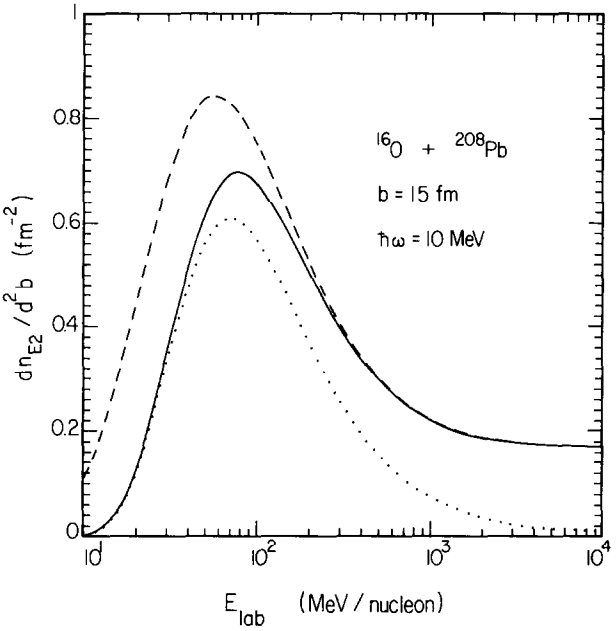

Fig. 3. Same as fig. 2, but for the E2 multipolarity.

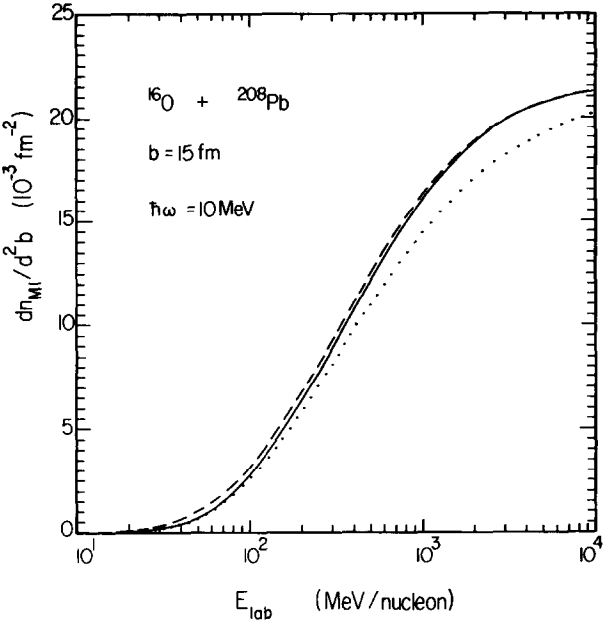

Fig. 4. Same as fig. 2, but for the M1 multipolarity.

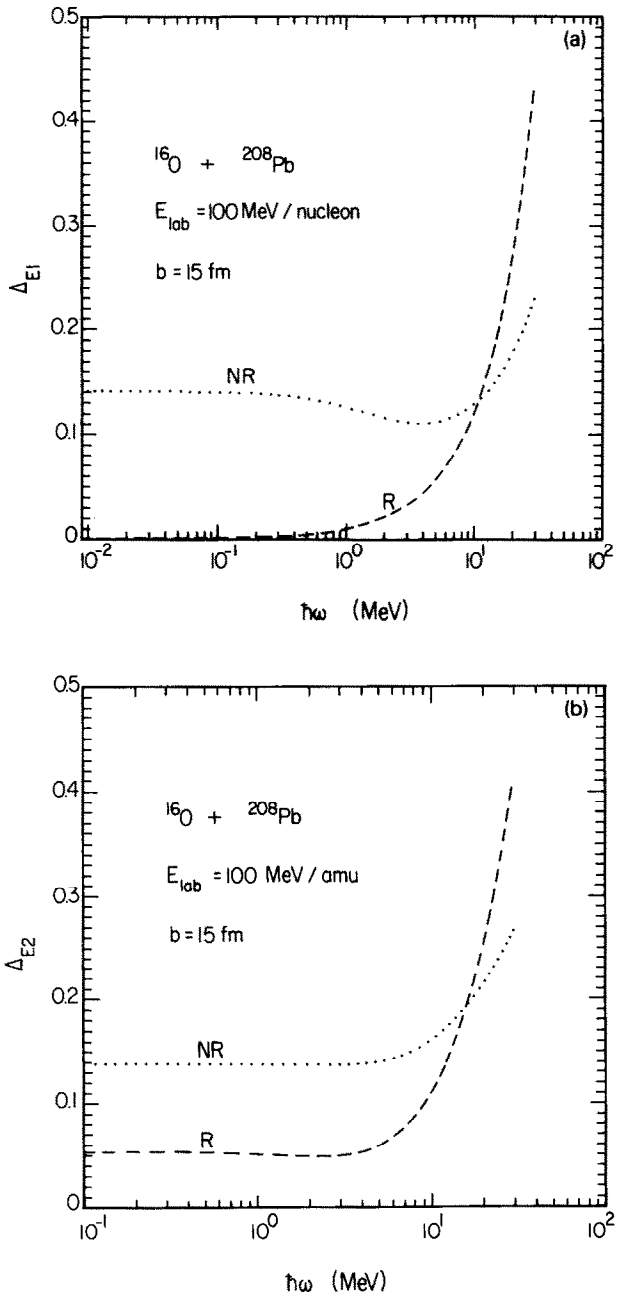

Fig. 5. Relative difference (see eq. (5.1)) between the non-relativistic (NR) and the relativistic (R) electric dipole number of equivalent photons per unit area, with the results calculated with the theory developed in text. We used $E_{lab} = 100$ MeV per nucleon and $b = 15$ fm in a $^{16}O + ^{208}Pb$ collision. Fig. 5b displays the same, but for the electric quadrupole multipolarity.

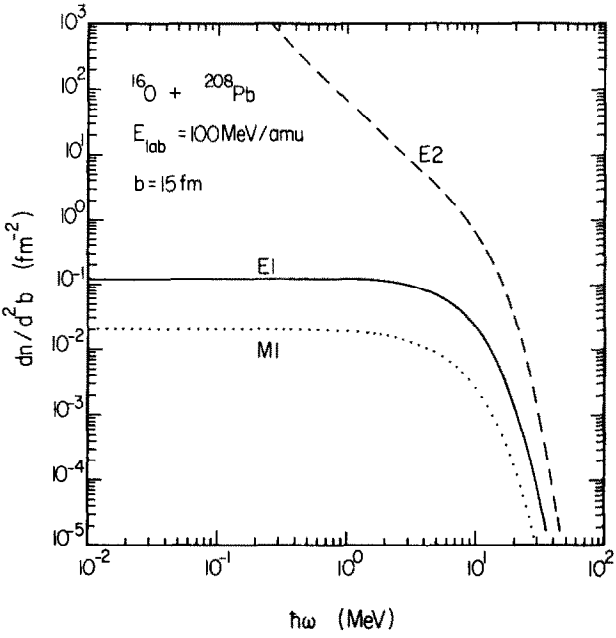

Fig. 6. Equivalent photon numbers per unit area incident on ^{208}Pb, in a collision with ^{16}O at 100 MeV per nucleon and with impact parameter $b = 15$ fm, as a function of the photon energy $\hbar\omega$. The curves for the E1, E2 and M1 multipolarities are shown.

the amplitudes obtained in the relativistic straight-line calculations with the amplitudes calculated non-relativistically in a collision with large angular momentum (i.e. for a hyperbolic orbit of large excentricity, with the same impact parameter). They showed that an improved expression for relativistic Coulomb excitation is obtained by the rescaling indicated by the formula (2.8). This rescaling is related to the recoil shift in the distance between the ions during the collision. For $t = 0$ the shift is a_0/γ. For $t < 0$ it is less, and for $t > 0$ larger. The factor $\frac{1}{2}\pi$ takes into account that the average shift is larger than a_0/γ. Thus by using $b + \pi a_0/2\gamma$ instead of b, the relativistic expressions could give improved results in intermediate-energy collisions [9]). In figs. 7 and 8 a comparison between the correct values and the relativistic expressions of the appendix, corrected with a rescaling of the impact parameter as indicated above, is displayed. The curves represent the percentual difference

$$\delta_{\pi\lambda}^{\text{correc}} = 100\{1 - \mathrm{d}n_{\pi\lambda}/\mathrm{d}n_{\pi\lambda}^{\text{correc}}\}\,, \tag{5.2}$$

where $\mathrm{d}n_{\pi\lambda}^{\text{correc}}$ are the relativistic equivalent photon numbers with "corrected" impact parameter.

In fig. 7 we show this percentual difference in a $^{16}O + ^{208}Pb$ collision with $b = 15$ fm and $\hbar\omega = 10$ MeV, as a function of the bombarding energy per nucleon. Fig. 8 displays the percentual error for the same collision, but with $E_{\text{lab}}/A = 100$ MeV,

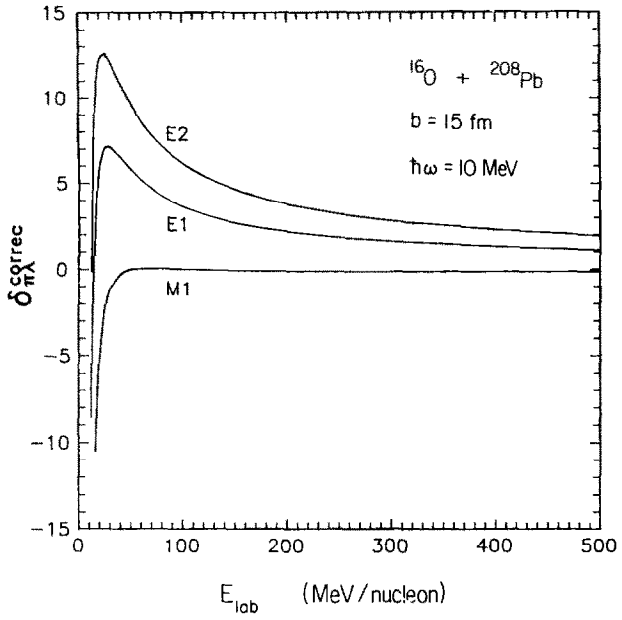

Fig. 7. Percentual difference (see eq. 5.2) between the equivalent photon numbers calculated with the theory developed in sect. 4 and the relativistic formulas of the appendix corrected for recoil. We take an $^{16}O + ^{208}Pb$ collision with $\hbar\omega = 10$ MeV and $b = 15$ fm.

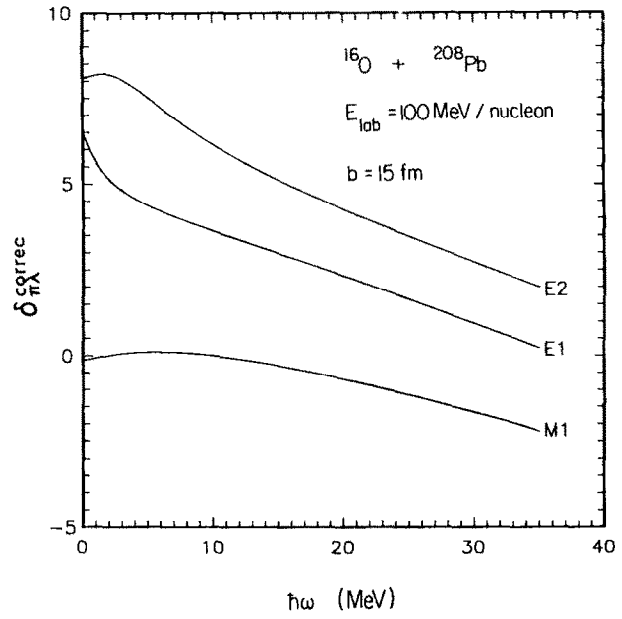

Fig. 8. Same as fig. 7, but for $E_{lab} = 100$ MeV per nucleon, and as a function of the excitation energy $\hbar\omega$.

and as a function of $\hbar\omega$. The difference is larger at low frequencies ω. At frequencies above 10 MeV the corrected expressions work very well. In both figures one sees that the M1 equivalent photon numbers are less sensitive to a more correct treatment of the orbital motion. As expected, the improved straight-line expressions are not very accurate for low-energy collisions, but work quite well for energies above 100 MeV per nucleon.

As an application of the semiclassical approach to Coulomb excitation in intermediate-energy collisions, we study the excitation of giant isovector dipole resonances (E1) and of giant isoscalar quadrupole resonances (E2) in ^{208}Pb by means of the Coulomb interaction with a ^{16}O projectile. At 100 MeV per nucleon the maximum scattering angle which still leads to a pure Coulomb scattering (assuming a sharp cutoff at an impact parameter $b = R_P + R_T$) is 3.9°. The cross sections are calculated by assuming a lorentzian shape for the photonuclear cross sections:

$$\sigma_\gamma^{\pi\lambda} = \sigma_m \frac{\varepsilon^2 \Gamma^2}{(\varepsilon^2 - E_m^2)^2 + \varepsilon^2 \Gamma^2}, \tag{5.3}$$

with σ_m chosen to reproduce the Thomas-Reiche-Kuhn sum rule for E1 excitations,

$$\int \sigma_\gamma^{E1}(\varepsilon)\, d\varepsilon \approx 60 \frac{NZ}{A} \text{ MeV} \cdot \text{mb} \tag{5.4a}$$

and the energy-weighted sum rule for the quadrupole mode,

$$\int \sigma_\gamma^{E2}(\varepsilon) \frac{d\varepsilon}{\varepsilon^2} \approx 0.22 Z A^{2/3} \mu\text{b/MeV}. \tag{5.4b}$$

The resonance energies are approximately given by $E_{GDR} \approx 77 A^{-1/3}$ MeV and $E_{GQR} \approx 63 A^{-1/3}$ MeV. We use the widths [10]) $\Gamma_{GDR} = 4$ MeV and $\Gamma_{GQR} = 2.2$ MeV for ^{208}Pb.

The cross sections increase rapidly with increasing scattering angle, up to an approximately constant value as the maximum Coulomb scattering angle is neared. This is explained as follows. Very forward angles correspond to large-impact-parameter collisions in which case $\omega b/\gamma v > 1$ and the excitation of giant resonances in the nuclei is not achieved. As the impact parameter decreases, increasing the scattering angle, this adiabaticity condition is fulfilled and excitation occurs. Also, the equivalent photon numbers vary slowly with b, in an interval from some tens of fermis down to the minimum grazing value. This explains the behaviour of fig. 9. It is seen that at 100 MeV per nucleon the excitation of the quadrupole mode dominates by a factor 2 over the dipole mode. But this could in fact be less if we had used the experimental values for the photonuclear cross reaction yields, which deplete about 60% of the energy-weighted sum rule [11]).

In fig. 10 is shown the total cross section for the excitation of giant dipole and of giant quadrupole resonances in ^{208}Pb in a collision with ^{16}O as a function of the laboratory energy per nucleon. The same average behaviour of the photonuclear

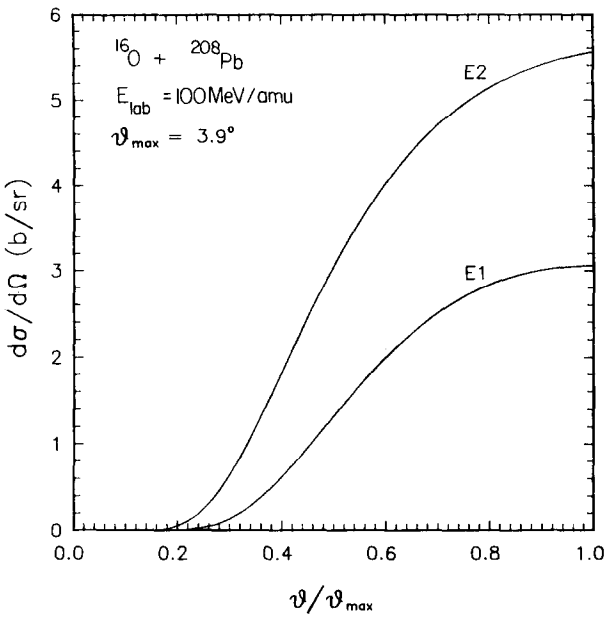

Fig. 9. Differential cross sections for the excitation of giant electric dipole (E1) and quadrupole (E2) resonances in ^{208}Pb by means of the Coulomb interaction with ^{16}O at 100 MeV per nucleon. ϑ_{max} is the maximum Coulomb scattering angle, which is about 3.9°.

cross sections, as assumed in eqs. (5.3) and (5.4), is used. The Coulomb excitation cross sections were obtained by an integration over the scattering angle up to the maximum value of pure Coulomb scattering. The cross sections increase very rapidly to large values, which are already attained at intermediate energies. A salient feature is that the cross section for the excitation of giant quadrupole modes is very large at low and intermediate energies, decreasing in importance (about 10% of the E1 cross section) as the energy increases above 1 GeV per nucleon. This occurs because the equivalent photon number for the E2 multipolarity is much larger than that for the E1 multipolarity at low collision energies. That is, $n_{E2} \gg n_{E1}$, for $v \ll c$. This has a simple explanation. Pictorially, as seen from an observator at rest, when a charged particle moves at low energies the lines of force of its corresponding electric field are isotropic, diverging from its centre in all directions. This means that the field carries a large amount of tidal (E2) components. On the other hand, when the particle moves very fast its lines of force appear contracted in the direction perpendicular to its motion due to Lorentz contraction. For the observator this field looks like a pulse of plane waves of light. But plane waves contain all multipolarities with the same weight, and the equivalent photon numbers become all approximately equal, i.e. $n_{E1} \approx n_{E2} \approx n_{M1}$, and increase logarithmically with the energy for $\gamma \gg 1$. The difference in the cross sections when $\gamma \gg 1$ are then approximately equal to the difference in the relative strength of the two giant resonances $\sigma_\gamma^{E2}/\sigma_\gamma^{E1} < 0.1$. The

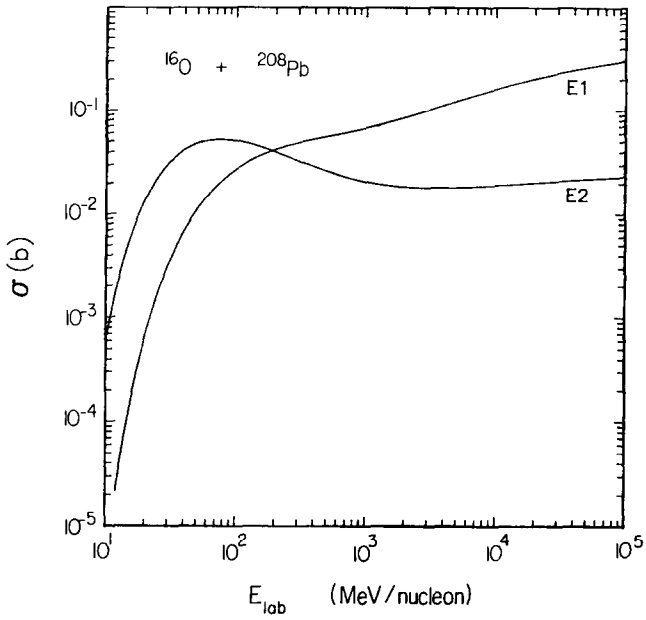

Fig. 10. Total cross sections for the excitation of giant electric dipole (E1) and quadrupole (E2) resonances in ^{208}Pb by means of the Coulomb interaction with ^{16}O, as a function of the laboratory energy.

excitation of giant magnetic dipole resonances is of less importance, since for low energies $n_{M1} \ll n_{E1}$ ($n_{M1} \approx (v/c)^2 n_{E1}$), whereas for high energies, where $n_{M1} \approx n_{E1}$, it will be also much smaller than the excitation of electric dipole resonances since their relative strength $\sigma_\gamma^{M1}/\sigma_\gamma^{E1}$ is much smaller than unity.

At very large energies the cross sections for the Coulomb excitation of giant resonances overcome the nuclear geometrical cross sections. Since these resonances decay mostly through particle emission or fission, this indicates that Coulomb excitation of giant resonances is a very important process to be considered in relativistic heavy-ion collisions and fragmentation processes, especially in heavy-ion colliders. At intermediate energies the cross sections are also large and this opens new possibilities to establish and study the properties of giant resonances [5]).

As a last remark, we point out that a study of the interplay of Coulomb repulsion and of retardation in Coulomb collisions at intermediate energies should also consider the fact that the intrinsic referentials of the two nuclei are non-inertial ones. Fewell [12]) has performed a study of these effects, although in low-energy collisions, and for back-scattering angles where the corrections are more important. His calculations are very elaborated, involving differential geometry, and aiming to find a hamiltonian for an accelerated system of charged particles in an external electromagnetic field. For some situations where first-order perturbation theory is applicable, he found that the corrections can exceed 10% from what one obtains by using the standard non-relativistic Coulomb excitation theory. At intermediate

energies, due to the fact that the scattering angle is limited to the very forward direction, we expect that effects from non-inertiality are not important. Nonetheless, this should be an interesting point for future investigations, and is a fascinating problem even in the classical context.

6. Conclusions

We developed an extension of the semiclassical theory of Coulomb excitation to include retardation effects in intermediate-energy collisions. For the scattering of a light by a heavy nucleus, one can quite straightforwardly use an analytical parametrization of the classical trajectory corrected relativistically. The retardation is included automatically by a multipole expansion of the retarded electromagnetic potential for a particle moving along such trajectory. Excitation amplitudes are then calculated within the semiclassical approach.

The Coulomb cross sections can be reduced to the cross sections for the corresponding photoreactions by using the idea of equivalent photons. Therefore, the measurement of Coulomb scattering is a complementary method to study photo cross sections and hence to reveal the nuclear structure. At intermediate and high energies, above 50 MeV/nucleon, mainly collective states of different multipole orders, like giant resonance states, are excited. Of great interest in experiments at these energies is the investigation of exotic decays of heavy target nuclei [4]). This could be accomplished through a multiple excitation of giant resonances, which can lead to very large collective motions of the nucleons, followed by an unusual decay of the nucleus.

We have shown that at intermediate energies discrepancies as large as 20% are obtained if one uses the low- or high-energy theories of Coulomb excitation. Such discrepancies should be considered in experiments with energies around 100 MeV per nucleon which are now becoming available [5]). The semiclassical approach outlined in the previous sections gives an improved solution to this problem.

One of the authors (C.A.B.) is very indebted to Prof. A. Winther and to Prof. G. Baur for useful discussions.

Appendix

Inserting the non-relativistic orbital integrals (3.9) into eq. (4.6), we get the following relation for the non-relativistic equivalent photon numbers (NR)

$$\frac{\mathrm{d}n_{\pi\lambda}^{\mathrm{NR}}}{\mathrm{d}\Omega} = Z_{\mathrm{P}}^2\alpha\frac{\lambda[(2\lambda+1)!!]^2}{(2\pi)^3(\lambda+1)}\,\zeta^{-2\lambda+2}\left(\frac{c}{v}\right)^{2(\lambda+\delta)}\frac{\mathrm{d}f_{\pi\lambda}}{\mathrm{d}\Omega}(\vartheta,\zeta) \tag{A.1}$$

where $\delta = 0$ for electric, and $\delta = -1$ for magnetic multipolarities, and $\zeta = \omega a_0/v$. The non-relativistic Coulomb excitation functions $f_{\pi\lambda}(\vartheta,\zeta)$ are very well known and e.g. are tabulated in ref. [1]) or may be calculated numerically.

The expression for the equivalent photon numbers in relativistic collisions is [4])

$$\frac{\mathrm{d}n^{\mathrm{R}}_{\pi\lambda}}{2\pi b\,\mathrm{d}b} = Z_{\mathrm{P}}^2\alpha\left(\frac{\omega}{\gamma v}\right)^2 \frac{\lambda[(2\lambda+1)!!]^2}{(2\pi)^3(\lambda+1)} \sum_{\mu} |G(\pi\lambda,\mu)|^2 K_{\mu}^2\left(\frac{\omega b}{\gamma v}\right), \tag{A.2}$$

where $G(\pi\lambda, \mu)[c/v]$ are the relativistic Winther–Alder functions, given analytically in ref. [3]) and K_μ is the modified Bessel functions of order μ.

For the E1, E2 and M1 multipolarities one finds

$$\frac{\mathrm{d}n^{\mathrm{R}}_{\mathrm{E1}}}{2\pi b\,\mathrm{d}b} = \frac{Z_{\mathrm{P}}^2\alpha}{\pi^2}\frac{\xi^2}{b^2}\left(\frac{c}{v}\right)^2\left\{K_1^2 + \frac{1}{\gamma^2}K_0^2\right\}, \tag{A.3a}$$

$$\frac{\mathrm{d}n^{\mathrm{R}}_{\mathrm{E2}}}{2\pi b\,\mathrm{d}b} = \frac{Z_{\mathrm{P}}^2\alpha}{\pi^2 b^2}\left(\frac{c}{v}\right)^4\left\{\frac{4}{\gamma^2}[K_1^2 + \xi K_0 K_1 + \xi^2 K_0^2] + \xi^2(2 - v^2/c^2)^2 K_1^2\right\}, \tag{A.3b}$$

$$\frac{\mathrm{d}n^{\mathrm{R}}_{\mathrm{M1}}}{2\pi b\,\mathrm{d}b} = \frac{Z_{\mathrm{P}}^2\alpha}{\pi^2}\frac{\xi^2}{b^2}K_1^2, \tag{A.3c}$$

where all K_μ's are functions of $\xi(b) = \omega b/\gamma v$. Improved expressions to describe Coulomb excitation in intermediate energy collisions, where Coulomb repulsion becomes as important as retardation, may be obtained by substituting $b \to b + \pi a_0/2\gamma$ in the above expressions.

References

1) K. Alder and A. Winther, Electromagnetic excitation (North-Holland, Amsterdam, 1975)
2) H. Heckman and P. Lindstrom, Phys. Rev. Lett. **37** (1976) 56
3) A. Winther and K. Alder, Nucl. Phys. **A319** (1979) 518
4) C.A. Bertulani and G. Baur, Phys. Reports **163** (1988) 299
5) F.E. Bertrand, J.R. Beene, and D.J. Horen, invited paper presented at Third Int. Conf. on nucleus–nucleus collisions, St. Malo, France, June 6–11, 1988, Nucl. Phys. **A488** (1988) 163c, and further references contained therein
6) G. Baur, C.A. Bertulani and H. Rebel, Nucl. Phys. **A458** (1986) 188
7) L.D. Landau and E.M. Lifshitz, The classical theory of fields, 4th ed. (Pergamon, Oxford, 1979) p. 93
8) M. Abramowitz and I.A. Stegun, Handbook of mathematical functions (National Bureau of Standards, Washington, 1964)
9) A. Winther, private communication
10) H.P. Morsch *et al.*, Phys. Rev. **C28** (1983) 1947
11) F.E. Bertrand *et al.*, Phys. Rev. **C34** (1986) 45
12) M.P. Fewell, Nucl. Phys. **A425** (1984) 373